# Characterization of CoCu- and CoMn-based catalysts for the Fischer Tropsch reaction toward chainlengthened oxygenates

Jenny Voss<sup>1</sup>, Yizhi Xiang<sup>1,3</sup>, Greg Collinge<sup>1</sup>, Danny Perea<sup>2</sup>, Libor Kovarik<sup>2</sup>, Jean-Sabin McEwen<sup>1,2,4,5</sup>, Norbert Kruse<sup>\*,1,2</sup>

<sup>1</sup>Voiland School of Chemical Engineering and Bioengineering, Washington State University, Pullman, WA 99164, USA

#### **Abstract**

The need for a sustainable energy supply in the face of depleting oil reserves has reignited the importance of Fischer Tropsch (FT) Synthesis technology. Presently, the FT process is practiced at the industrial scale to predominately produce synthetic diesel-type fuels and lubricants. More recently, the possibility of hydrogenating CO toward oxygenates, and not just hydrocarbons, has been explored. We have developed a series of CoCuMn and CoMnK catalysts prepared via the oxalate co-precipitation route that are capable of forming oxygenates with desirable selectivity. Upon H<sub>2</sub>-assisted thermal decomposition of the resultant mixed metal Co<sub>1</sub>Cu<sub>1</sub>Mn<sub>1</sub> oxalates, catalysts naturally exhibited a cobalt core-copper shell configuration with Mn<sub>5</sub>O<sub>8</sub> throughout the catalyst nanoparticle as determined via Atom Probe Tomography (APT). We suggest structural changes are induced by the CO and H<sub>2</sub> reactants to form the catalytically active phase under real-time reaction conditions as demonstrated by corroborative density functional theory calculations and experimental evidence. APT studies also show that a Co<sub>4</sub>Mn<sub>1</sub>K<sub>0.1</sub> catalyst post reaction contained a cobalt carbide phase as determined from a Co/C ratio of 2/1. Manganese and potassium were found only in the outermost part of the particle. Both catalysts were found to contain the presence of a Mn<sub>5</sub>O<sub>8</sub> oxidic phase before and post reaction which we attribute to the high activity toward oxygenates of these two catalysts.

**Keywords:** Fischer Tropsch, oxygenates, atom probe tomography, Co-based catalysts, Cobalt carbide

<sup>&</sup>lt;sup>2</sup> Institute for Integrated Catalysis, Pacific Northwest National Laboratory, Richland, Washington 99332, USA

<sup>&</sup>lt;sup>3</sup>Dave C. Swalm School of Chemical Engineering, Mississippi State University, MS State, Mississippi 39762, USA

<sup>&</sup>lt;sup>4</sup>Department of Chemistry, Washington State University, Pullman, WA, 99164, USA

<sup>&</sup>lt;sup>5</sup> Department of Physics, Washington State University, Pullman, WA, 99164, USA

<sup>\*</sup>Corresponding Author email: norbert.kruse@wsu.edu

### 1. Introduction

In the breadth of the early 1920's, two scientists by the name of Franz Fischer and Hans Tropsch at the Kaiser Wilhelm Institut für Kohlenforschung in Mülheim an der Ruhr, Germany, observed the catalytic reaction of H<sub>2</sub> and CO to produce hydrocarbons and oxygenates [1]. Different from the original patent by BASF (Badische Anilin und Soda-Fabrik) in 1913 [2], they realized that chain-lengthened products contain multiple -CH<sub>2</sub>- units and therefore need H<sub>2</sub>/CO ratios larger than one. With the depletion of natural oil reserves and the need for a sustainable energy supply, the Fischer-Tropsch (FT) synthesis has regained importance over the recent past. It is being practiced on the industrial scale to mainly produce diesel-type fuels and lubricants with straight-chained hydrocarbons [3].

More recently, the possibility has been explored to hydrogenate CO toward oxygenates instead of hydrocarbons. The Fischer-Tropsch synthesis is thereby used as a vehicle for hydrocarbon chain lengthening. The manufacturing of short-chain alcohols ("higher alcohols") is driven by incentives to produce transportation fuel additives and building blocks for the polymers industry. Likewise, fatty alcohols and aldehydes are interesting for use as lubricants, detergents and plasticizers. The selective synthesis of long-chain oxygenates is a kinetic problem since the thermodynamics are favorable [4]. The formation of oxygenates is favored by low temperatures where the entropic contributions to the Gibbs energy are not as important. With growing hydrocarbon chain length of the alcohol, the Gibbs free energy becomes more negative [5]. The major challenge with selectively forming long-chain alcohols (Eq. 1) via the FT reaction is the kinetic competition with formation of paraffins (Eq. 2), olefins (Eq. 3) and other side reactions (see equations below). Consequently, catalysts must be designed to achieve structure – selectivity relationships that favor hydrocarbon chains with terminal oxygen functionality over linear saturated hydrocarbons. Moreover, the methane formation via the Sabatier reaction (Eq. 4) and CO<sub>2</sub> formation via water gas shift (Eq. 5) and the Boudouard (Eq. 6) reactions have to be kept under control.

$2nH_2 + nCO \to C_nH_{2n+1}OH + (n-1)H_2O$	Equation 1
$(2n+1)H_2 + nCO \rightarrow C_nH_{2n+2} + nH_2O$	Equation 2
$2nH_2 + nCO \rightarrow C_nH_{2n} + nH_2O$	Equation 3
$3H_2 + CO \rightarrow CH_4 + H_2O$	Equation 4
$CO + H_2O \leftrightarrow CO_2 + H_2$	Equation 5
$2\ CO \rightarrow CO_2 + C$	Equation 6

Various types of catalysts have been developed to transform H<sub>2</sub> and CO into oxygenated hydrocarbons. The most notable catalysts include Rh, MoS<sub>2</sub> and modified FT CoCu ones [6]. Ruthenium-based catalysts are favored for synthesis of ethanol and other C<sub>2</sub>+ oxygenates such as acetic acid and acetaldehyde [7, 8]. The rarity and expense of the element renders it incompatible with large scale FT applications. Molybdenum sulfide (MoS<sub>2</sub>) catalysts have found success in the formation of long chain alcohols [9, 10]. However, MoS<sub>2</sub> catalysts typically need to be regenerated with sulfur which is not ideal considering sulfur typically poisons other catalysts used in downstream separation at refineries and other chemical plants. Here on, we focus on the development of modified Fischer Tropsch CoCu and CoMn catalysts for the synthesis of long chain alcohols and aldehydes, respectively. Other reviews are available for alternate catalysts considered for higher alcohol formation [6, 11–17]. After a short introduction into "early times" research of higher alcohol formation through CO hydrogenation, we will mainly develop aspects of relevant structural and compositional properties of CoCu- and CoMn-based catalysts on the basis

of experimental investigations using 3D Atom-Probe Tomography (APT), Transmission Electron Microscopy (TEM) and theoretical calculations by Density Functional Theory (DFT).

## 2. Development of modified CoCu and CoMn Catalysts for Oxygenates Formation

The concept of oxygenated hydrocarbons ("higher alcohols") using FT Synthesis technology was first pioneered by the "Institut Français du Petrole" (IFP) in the late 1970's and early 1980's. IFP brought to light the possibility of manufacturing  $C_1 - C_6$  alcohols for use in motor fuels using CoCu catalysts [18]. Designs of CoCu catalysts were adjusted so that higher alcohols were obtained under comparable operational conditions of pre-existing methanol processes while favoring desired alcohol length and selectivity [6]. Typical IFP catalysts contained cobalt, copper, at least one metal oxide and an alkali metal promoter [19]. Yet, catalyst preparation remained ambiguous and sometimes lacked reproducibility leaving much skepticism in the community up until now.

Within recent years, a series of CoCu- and CoMn-based catalysts were prepared via oxalate precursors (see paragraph 3.2) by Xiang et al. [20, 21]. Both long- and short-chained alcohols and aldehydes were found to form at favorable selectivities. The addition of metal oxides tuned the behavior of the CoCu catalysts in terms of water gas shift activity (WGS), CO conversion and selectivity toward alcohols and olefins [20]. Most notably, long-chain alcohols were synthesized by a "CoCuMn" catalyst (atomic amounts of elements in this case: 1:1:1; however, other relative compositions were also investigated) containing a Mn promoter/dispersant in the form of Mn<sub>5</sub>O<sub>8</sub> [22]. In the absence of Cu, CoMn was found to form alcohols as well as aldehydes [21]. Further addition with potassium, usually considered a "structural" promoter, resulted in a CoMnK catalyst that strongly favored selectivity toward aldehydes using feeds with low H<sub>2</sub>/CO ratios [21]. Exchanging K for a Li promoter, i.e. employing CoMnLi catalysts, turned out to form appreciable amounts of olefins [21]. Quite clearly, addition of metal oxide and alkali promoters are valuable tools for tuning selectivity to desirable oxygenates and olefins (the latter being interesting high-value products, too).

### 3. The Nature of CoCu- and CoMn-based catalysts

CoCu-based catalysts for higher alcohol synthesis via CO hydrogenation are frequently considered to combine both Fischer Tropsch chain lengthening (Co) and water gas shift (Cu) properties. This (oversimplifying) picture is occasionally extended to associating Co metal to be responsible for CO dissociation and the Cu metal to keep the CO molecule intact. We note that while there is no doubt that a stepped Co surface can dissociate the C-O triple bond there is presently neither experimental nor theoretical proof that the chain lengthening mechanism to produce oxygenates involves C-C coupling of (partially hydrogenated) surface carbon atoms. Instead, a CO insertion mechanism may be a serious option to explain both chain growth and oxygen functionalization. One has to keep in mind that both metals show only limited miscibility, see below Figure 1. There is, however, no doubt about a synergy effect between these two elements resulting in a catalyst which produces chain-lengthened hydrocarbons with terminal alcohol functionality.

Alkali metal promoted CoMn- differ from CoCu-based catalysts by forming both alcohols and aldehydes. It has been suggested that the presence of an alkali metal, especially K, promotes the reconstruction of the active catalytic phase during the induction period of the reaction. Such reconstruction results in the formation of bulk Co<sub>2</sub>C dispersed by a Mn<sub>5</sub>O<sub>8</sub> oxidic phase with Mn<sup>2+</sup> and Mn<sup>4+</sup> mixed valence states [21]. The Mn<sub>5</sub>O<sub>8</sub>-Co<sub>2</sub>C interface is presently advocated as being essential for the formation of the active sites of oxygenates production. Similar conclusions were also drawn in other literatures when focused on the synthesis of short-chain olefins from FT synthesis [23]. It should be emphasized, however, that the atomic configurations of "active sites" for oxygenate and/or olefin production are not known at present. Yet it seems they differ from those that are relevant for saturated hydrocarbon production.

## 3.1. Structural and compositional analysis of CoCu- and CoMn-based catalysts

A number of fundamental questions regarding the very nature of CoCu-based catalysts have been raised throughout the literature. Co is accepted to be responsible for hydrocarbon chain growth whereas the role of Cu is not yet clear [24]. As seen in Figure 1 below, the metallic phase of an activated CoCu-based catalyst (actually a "CoCuMn" hybrid), prepared according to the oxalate route (see paragraph 3.2) in our laboratory, is core-shell structured. Atom Probe Tomography (APT) clearly reveals the low miscibility of cobalt and copper giving rise to a cobalt core – copper shell (Co@Cu) structure (before reaction). Indeed, one would expect copper to be surface-enriched since it has a lower Gibbs Free Surface Energy as compared to cobalt [24]. The oxalate route of catalyst preparation obviously favors self-assembling of Co and Cu atoms in a Co@Cu configuration.

As to the details of Figure 1, the occurrence of Cu in the core and, vice versa, of Co in the shell, are rather limited. Counting Cu atoms in the Co core leads to concentrations reflecting the thermodynamic maximum of 9% miscibility of Cu into Co [25]. Conversely, Co atoms are also present in the Cu-dominated shell. Atoms of Mn are dispersed throughout in both the shell and core of the nanoparticle, occasionally appearing as precipitates. Atoms of O are found in the shell of the nanoparticle. This is expected since the CoCuMn catalyst must be passivated by oxygen chemisorption after thermal oxalate decomposition due to the pyrophoric nature of the material. Since Me-O (metal-oxygen) surface species may undergo preferential field evaporation during the initial stages of the APT analysis, we suspect that the actual amount of oxygen atoms appearing in Figure 1 is underrepresented.

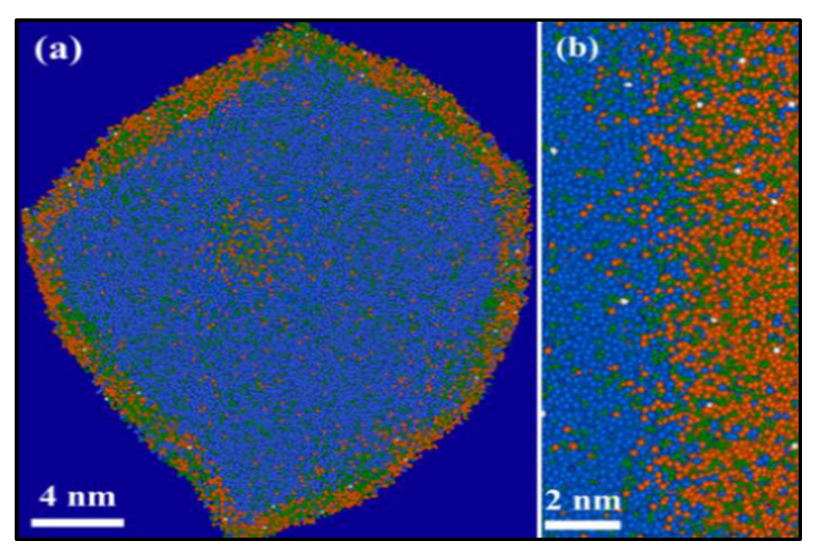


**Figure 1.** Atom Probe Tomography (APT) Reconstruction of a single CoCuMn nanoparticle catalyst after thermal decomposition of the mixed metal CoCuMn oxalate before experiencing CO hydrogenation. The data is presented in the form of an atomic resolution map in which Co atoms are depicted in blue spheres, Cu atoms as orange spheres, Mn atoms as green spheres and O atoms as white spheres. The displayed images show (a) a  $\sim$ 22 nm thick slice through one grain of a nanoparticle, and (b) an enlarged 6 nm thick view of the core-shell interface at the outskirts of the nanoparticle shell.

It is unlikely that the Co@Cu,Mn core-shell nature of the CoCuMn particle remains intact during the reaction. Even though an after-reaction APT analysis is not yet available, density functional theory (DFT) and X-ray Photoelectron Spectroscopy (XPS) show a CO-induced restructuring in a CoCu model catalyst [26]. Before demonstrating the result of swapping Cu for Co atoms in the presence of adsorbed CO, it is instructive to consider the experimental results obtained for inverse Cu@Co core-shell structures. The groups of Somorjai and Spivey both investigated synthetically manufactured Cu@Co core-shell nanoparticles [27–29]. Exposing such particles to both oxidizing and reducing atmospheres revealed the tendency for Cu to segregate to the surface in oxidizing atmospheres [27]. Once the Co@Cu configuration was reached, it remains stable when exposing it to H<sub>2</sub>. This suggests that Co@Cu core-shell nanoparticles are stable under environmental and net vacuum conditions which is in agreement with the APT results presented above and the DFT calculations in the absence of adsorbates (see Figure 2).

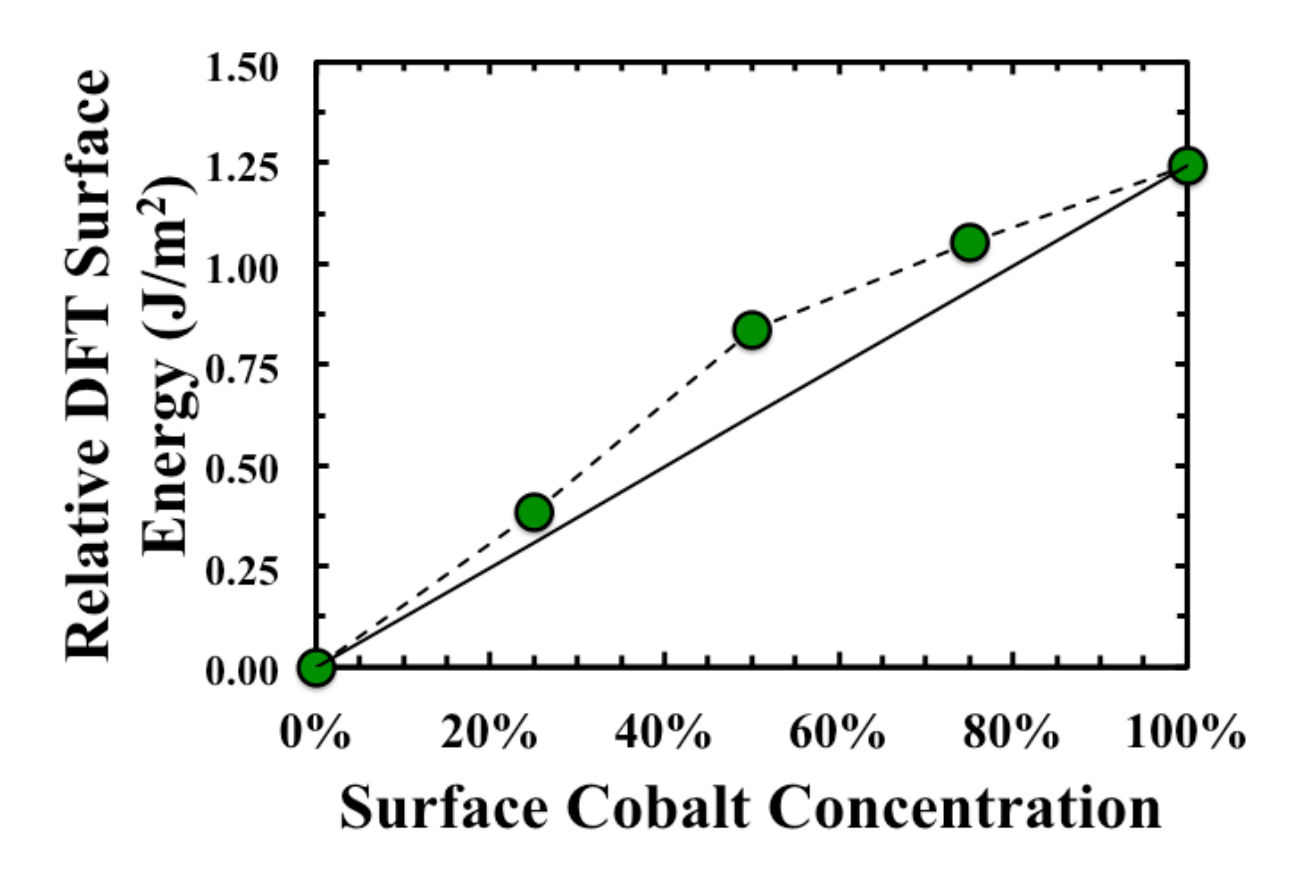


**Figure 2.** Dashed line: Minimum DFT surface energies of a  $p(2\times2)$  Cu/Co(0001) surface in vacuum as a function of surface Co concentration. The values show a clear preference for the Cu terminated system. The solid line shows the ideal DFT energy of mixing for visual reference.

Based on the experimental literature, it can be posited quite reasonably that the presence of adsorbed CO will cause surface reconstruction of as-prepared CoCu catalysts. Specifically testing the surface prevalence of Co on the Cu/Co(0001) surface, Figure 3 shows the extent to which this can be expected. The lowest DFT surface energies are found when 0.75 ML of CO (green triangles in Figure 3) are adsorbed in mixed on-top and triple-bridged positions on a surface terminated with a 100% Co surface layer. In fact, at 0.5 and 0.75 ML of CO, the surface energy is rather flat from 25% to 100% surface Co enrichment. Remarkably, fairly low CO surface coverages cause Cu to swap against Co and that the amount of surface Co varies non-linearly with the CO coverage. Furthermore, it is quite interesting to state that the p(2x2) reconstructed surface is more stable at 0.5 ML of CO than the same surface at 0.25 ML of CO. In both cases, p(2x2) overlayer structures are formed with Co(CO)<sub>2</sub> configurations in the former case and on-top CO positions in the latter case, respectively. Our theoretical results of a CO-induced reconstruction are also in agreement with earlier reports by Falo et al. [31] and Cerenco et al. [32] according to which CoCu nanoparticles suffer surface enrichment in Co and depletion in Cu under syngas exposure.

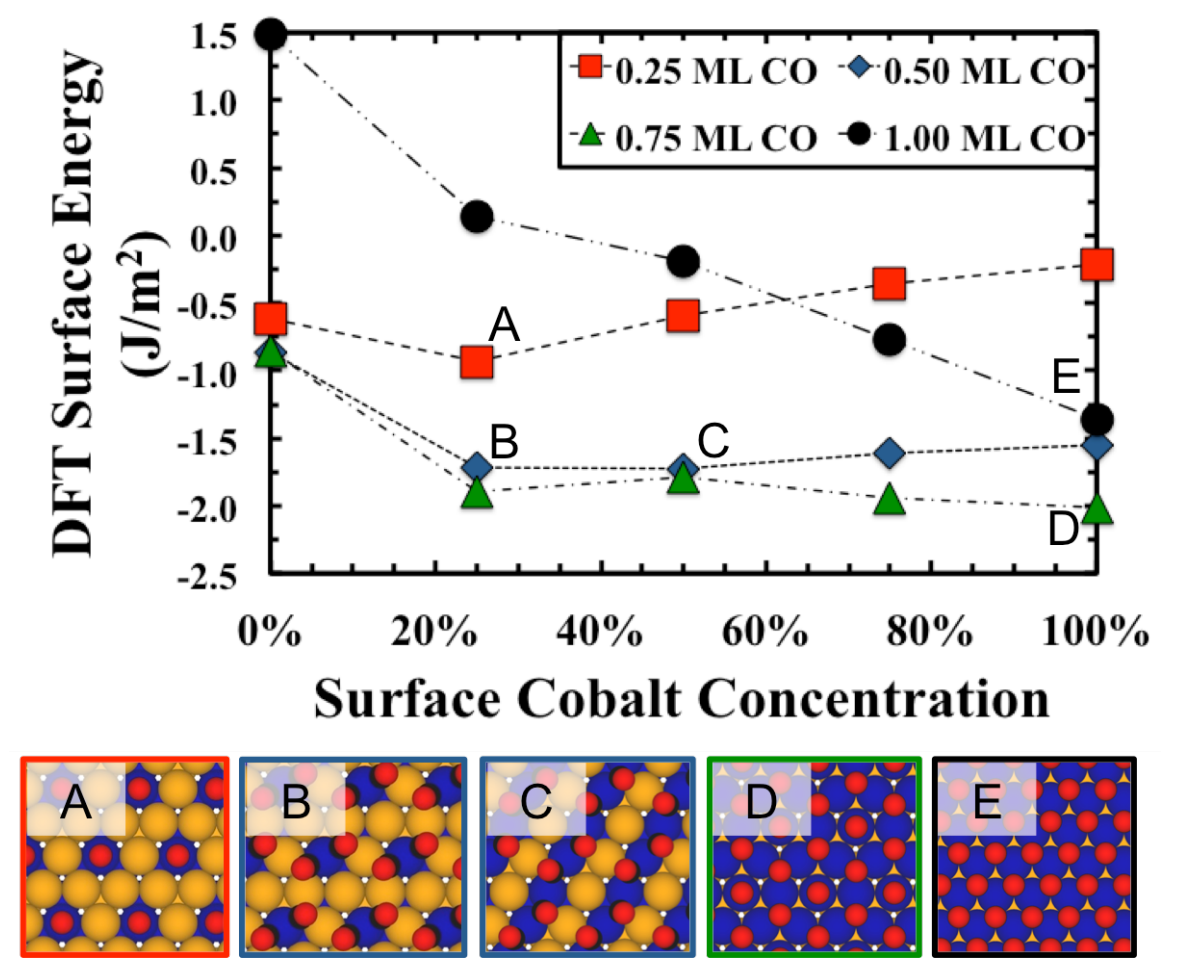


**Figure 3.** Minimum DFT surface energies of a Cu/Co(0001) surface as a function of CO coverage and surface Co concentration. The structures labeled A-E are top-down views of the minimum-energy CoCu configurations. The 0.50 ML CO case (blue diamonds) has two minimum-energy configurations (B and C) while the remainder have distinct ones. The blue spheres are Co, the orange spheres are Cu and the red spheres are O atoms of CO molecules binding via the Co atom to the surface.

When turning to CoMn-based catalysts in the absence of Cu, less information is presently available about the virgin metallic phase. Therefore, the question for the possible existence of a core-shell structure as encountered for CoCu and CoCuMn catalysts has to be postponed. On the other hand, a common feature of Mn-containing catalysts, i.e. CoCuMn and CoMnK, is the simultaneous occurrence of a Mn<sub>5</sub>O<sub>8</sub> phase in which Mn is present in both 2+ and 4+ valence states. Recently, we demonstrated by post-reaction TEM analysis that CoMnK catalysts, favoring long chain aldehydes at low CO/H<sub>2</sub> ratios, contain a stable Mn<sub>5</sub>O<sub>8</sub> phase (see Figure 4) [21, 30]. Furthermore, cobalt went from a metallic phase the before reaction to a cobalt carbide (Co<sub>2</sub>C) phase after the reaction. This was somewhat unexpected considering earlier characterization studies clearly showed Co remained in a metallic state during the catalytic reaction [24]. In the meantime, a reaction-induced Co<sub>2</sub>C phase has been reported and considered by several laboratories to contribute to alcohol formation in promoted Co and CoCu catalysts [21, 31–34]. Other competing reports for CoCu catalysts argued that the presence of Co<sub>2</sub>C may inhibit oxygenate functionality [26, 34, 35]. Furthermore, Co<sub>2</sub>C nanoprisms have been supposed to be responsible for lower olefins production [23]. The presence of Co<sub>2</sub>C has also been attributed to elevated methane formation [36]. Regardless of competing literature, we demonstrate by XRD (Figure 4) that CoMnK catalysts undergo a reaction-induced

transformation into a catalyst containing a Co<sub>2</sub>C phase along with a Mn<sub>5</sub>O<sub>8</sub> phase which are most probably in intimate contact so as to develop the active sites responsible for long-chain aldehyde/alcohol formation.

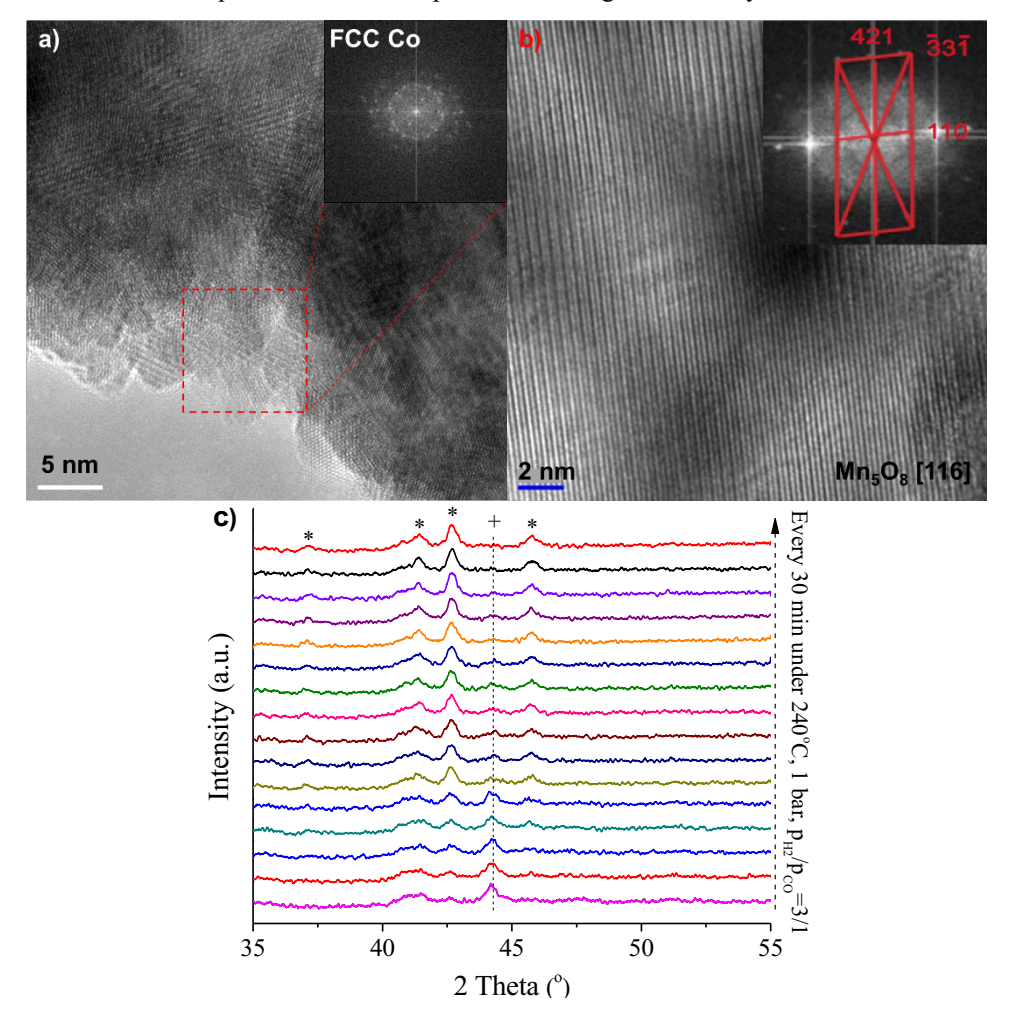
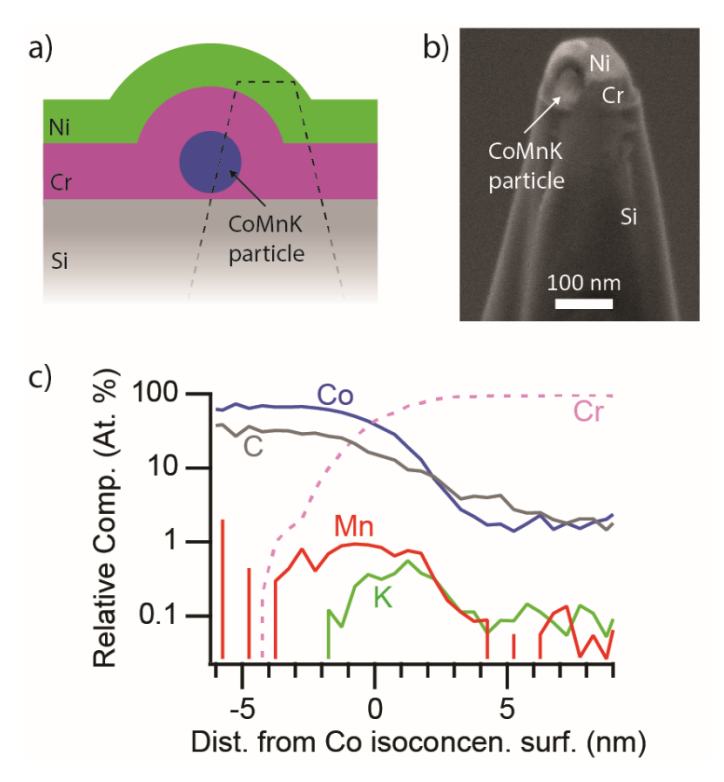


Figure 4. a) and b): (HR)TEM demonstrating Co (fcc) and  $Mn_5O_8$  occur in fresh (passivated)  $Co_4Mn_1K_{0.1}$  catalysts. c): in-situ XRD patterns of the same catalyst under atmospheric syngas conditions at  $H_2/CO = 3/1$  and  $240^{\circ}C$ . (\*)  $Co_2C$ , and (+) fcc Co.

We now turn to a preliminary APT composition profile of a Co<sub>4</sub>Mn<sub>1</sub>K<sub>0.1</sub> catalyst previously subjected to the Fischer Tropsch reaction (see Figure 5). The catalyst had to be passivated by oxygen chemisorption before subjecting it to APT. Because of the delicate sample preparation and the easy fracture of the samples under conditions of high electric fields in APT, individual catalyst nanoparticles were first deposited on a Si needle specimen and then covered by Cr (and Ni) serving as internal reference and field desorbing at low field strength (see Figure 5a,b). The embedded nanoparticles were then shaped into a sharp APT tip (less than 100 nm) using a technique known as SEM-FIB (Scanning Electron Microscopy – Focus Ion Beam) developed by K. Thompson et al. [37]. This technique was originally designed to prepare bulk phase specimens for APT analysis, rather than nanoparticles. Different from Figure 1, which shows a cross-sectional atom map of a nanosized Co<sub>1</sub>Cu<sub>1</sub>Mn<sub>1</sub> particle, we show here the concentration profiles for selected elements following layer-by-layer field evaporation of a Co<sub>1</sub>Mn<sub>1</sub>K<sub>0.1</sub> particle (Figure 5c). Obviously, when uncovering this particle through continuous field evaporation of the Cr reference (moving from right to left along the x-axis in Figure 5c), cobalt (Co) and carbon (C) are mainly field evaporated until a Co/C=2/1 ratio is reached for the bulk. This is in accordance with the occurrence of a Co<sub>2</sub>C phase. Furthermore, low concentrations of manganese and potassium are detected in the outer layers of the particle.

Note that these elements are essentially absent in the Co<sub>2</sub>C bulk. From this, we would suggest that an originally core-shell structured particle transforms into Co<sub>2</sub>C during the reaction and maintains low concentrations of Mn and K in the outermost layers of the particle. Such a Co@Co,Mn,K core-shell structure would ensure that all elements are in intimate contact so as to provide the unique catalytic properties of CoMnK catalysts in the FT synthesis to chain-lengthened aldehydes/alcohols. Our present efforts concentrate on capturing and analyzing full catalyst particles (rather than a fraction of it, as in Figure 5). These efforts include the need to elucidate the role of Mn<sub>5</sub>O<sub>8</sub> structures as revealed by TEM.



**Figure 5.** Atom Probe Tomography analysis of an individual Co<sub>4</sub>Mn<sub>1</sub>K<sub>0.1</sub> nanoparticle. a) Schematic representation showing a Co<sub>4</sub>Mn<sub>1</sub>K<sub>0.1</sub> nanoparticle embedded within Cr with a Ni capping layer on top of a Si substrate. b) FIB-prepared needle specimen analyzed by APT. The specimen geometry is outlined by the dashed shape in a). c) Proximity histogram composition profile of the specimen portraying the interface between the chromium embedding material and the Co<sub>4</sub>Mn<sub>1</sub>K<sub>0.1</sub> nanoparticle interface. The histogram stems from counts of atoms at defined distance from a cobalt rich (isoconcentric) region in the APT experimental data. From right (+) to left (-) of the Co isosurface, bulk Cr embedding material is abundant followed by a decrease in Cr and increase as elemental amounts of Co, C, Mn and K increase correlating to a transition into the Co<sub>4</sub>Cr<sub>1</sub>K<sub>0.1</sub> nanoparticle.

#### 3.2 CoCu- and CoMn-based catalysts via oxalate co-precipitation: key to self-assembled core-shell structures

Mixed-metal oxalate precursors as prepared in our laboratory contain no generic support material. Binary CoCu catalysts, despite proving constant steady-state activity and selectivity for more than 24h time-on-stream under FT reaction conditions [27], may suffer long-term performance stability. For CoCuMn and CoMnK catalysts, no such loss in performance was ever found during more than 78 h time-on-stream. The remarkable performance stability of these catalysts is likely due to the generation of an oxide phase, here Mn<sub>5</sub>O<sub>8</sub>, during the thermal decomposition of the ternary oxalate precursors.

Non-supported CoCu catalysts derived from the decomposition of a mixed-metal CoCu oxalate, a type of metal-organic-framework (MOF) structure, naturally exhibit a nanosized Co@Cu core-shell configuration [26].

150

8000

7000

Thus, a phase separation occurs during oxalate decomposition (see Figure 6). It is important to note that this phase separation does not involve Co and Cu to nucleate and grow into separate metal particles. H<sub>2</sub>-assisted Temperature Programmed Decomposition (H<sub>2</sub>-TPDec) clearly shows that the decomposition temperatures for co-precipitated CoCu oxalates are very different from those of the individual metal oxalates, CoC<sub>2</sub>O<sub>4</sub> and CuC<sub>2</sub>O<sub>4</sub> [27]. This is particularly true for mixed oxalates with Co/Cu atomic ratios larger than one (see Figure 6). Conversely, for Co/Cu ratios <1, the low temperature feature (265 °C) was observed to intensify. This can be straightforwardly correlated with the occurrence of CuC<sub>2</sub>O<sub>4</sub> decomposition. Note that the Co analogue, if present, would have been expected to appear at temperatures of around 375 °C. Its absence in Figure 6 provides further yet indirect proof of a CoCu oxalate co-precipitate containing both Co and Cu along with chelating oxalate groups, in a polymeric MOF structure. The fact that mainly CO<sub>2</sub> is formed during TPDec demonstrates that the activated catalyst is metallic.

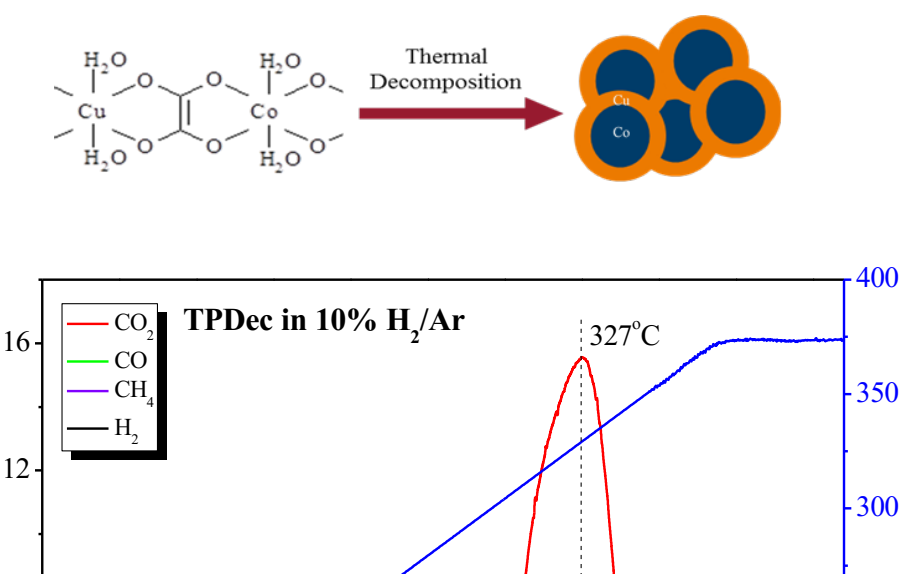


**Figure 6.** Hydrogen-assisted Thermal Decomposition of a mixed metal Co<sub>2</sub>Cu<sub>1</sub> oxalate results in nanosized CoCu catalyst particles that self-assemble into a Co@Cu core-shell configuration (see Figure 1). The chelating oxalate ligand is "burnt" off during the decomposition releasing CO<sub>2</sub> and CO molecules (minor). The activated catalyst is therefore largely in a metallic state. The temperature was ramped from room temperature to 375 °C at a rate of 3 °C/min using a flow of 10% H<sub>2</sub> in Ar.

277°C

Time (s)

6000

240°C

5000

4000

Outlet flow  $(vmol/g_{oxalate}/s)$ 

8

4

3000

For ternary CoCuMn and CoMnK catalyst precursors, the thermal decomposition profiles change quite substantially as compared to binary CoCu ones [20, 38]. Besides a metallic core-shell structured phase (see Figure

1), an oxidic phase, Mn<sub>5</sub>O<sub>8</sub>, is formed during TPDec. The decomposition (simplified by considering only Mn) therefore reads:

$$5MnC_2O_4 \rightarrow Mn_5O_8 + 8CO + 2CO_2$$

Equation 7

Consequently, considerable amounts of CO appear in the TPDec spectrum, the ratio of CO/CO<sub>2</sub> thereby roughly being in agreement with the stoichiometry of the decomposition, if the atomic composition of the actual CoCuMn catalyst is taken into account.

In summary, the oxalate route of catalyst preparation has proven to be simple, fast and reliable. Characterization of as-prepared oxalates by TPDec or XPS allowed distinguishing between metallic and oxidic phase formation [39]. Cutting-edge methods like APT and Scanning Transmission Electron Microscopy (S)TEM revealed the structural and compositional details of the catalysts before and after reaction. This is an important step toward an elucidation of the chemical nature of the catalytically active phase, a prerequisite for developing realistic mechanistic concepts of the FT reaction.

# 5. Concluding Remarks

Under optimal conditions, CoCuMn catalysts favor long chain alcohols whereas CoMnK catalysts favor long chain aldehydes. The role of Mn is at least twofold: it may act as a dispersant and as a promoter. It may coexist with other metals in core-shell metallic structures and as a  $Mn_5O_8$  oxidic phase which we consider key to increased oxygenate functionality of the catalysts. CoMnK catalysts favoring higher aldehydes developed a  $Co_2C$  phase during the reaction where the  $Mn_5O_8$  promoter remained stable.

Cutting edge techniques, such as Atom Probe Tomography, demonstrated CoCuMn catalysts naturally exhibit a Co@Cu,Mn core-shell structure. STEM demonstrated concomitant Mn<sub>5</sub>O<sub>8</sub> clusters remained highly dispersed throughout the catalyst so as to guarantee high specific surface areas during reaction. Both density functional theory and experimental XPS findings agree that CoCu catalysts undergo significant reconstruction under reactive conditions. Determining the catalytically active phase responsible for alcohol formation is vital for the targeted design of such catalysts and still remains a challenge today.

Comparatively, CoMnK catalysts favoring formation of oxygenates – mainly aldehydes – also underwent significant reconstruction. Cobalt in the CoMnK catalyst originally existed in a metallic state which was then transformed into a Co<sub>2</sub>C phase as determined by in-situ and post reaction XRD analysis. The APT post reaction analysis of this catalyst demonstrates a cobalt carbide phase to be formed along with a surface layer containing all three elements, Co, Mn and K, The APT method has therefore demonstrated its unique capability of providing chemical maps of atoms, with unprecedented lateral resolution, across the bulk of individual nanoparticles.

The oxalate co-precipitation route used in our laboratory allows the mixing of Co, Cu and Mn metals into a common polymeric MOF structure. This technique bypasses bulk miscibility limits by locking metal ions in neighboring positions via chelating oxalate ligands. No generic support material is needed when preparing catalysts through oxalate precursors. The necessary metal-metal oxide systems form through temperature-programmed decomposition of oxalate precursors. As we demonstrated, this unique synthesis route allows mixing of metal ions at the instant of precipitation thereby creating synergies between elements which may be difficult to achieve via more classical methods of catalyst preparation. We anticipate that the oxalate route of catalyst preparation will enjoy further applications in the future. The CoCuMn and CoMnK examples investigated here in relation to higher oxygenates' synthesis are highly encouraging.

### Acknowledgements

J.-S.M. and N.K. were supported by the National foundation under contract no. CBET-1438227. G.C. was supported by the National Science Foundation Graduate Student Fellowship Program under contract number 1347973. J.V. was also supported by the National Science Foundation Graduate Student Fellowship Program. G.C. and J.V, Seattle Chapter ARCS Fellows, gratefully acknowledge financial support from the Achievement Rewards for College Scientists foundation. J.V. acknowledges the support of the U.S. Department of Energy, Office of Science Graduate Student Research program administered by the Oak Ridge Institute for Science and Education (ORISE) which is managed by ORAU under contract number DE-SC0014664. A portion of the research was performed using EMSL, a national scientific user facility sponsored by the Department of Energy's Office of Biological and Environmental Research and located at PNNL. PNNL is a multiprogram national laboratory operated for the U.S. DOE by Battelle.

#### References

- 1. Fischer F, Tropsch H (1926) Über Die Direkte Synthese von Erdöl-Kohlenwasserstoffen Bei Gewöhnlichem Druck.(Erste Mitteilung). Eur J Inorg Chem 59:830–831
- 2. BASF (1913) Und Soda-Fabrik, Ludwigshafen a. German Patent DE 2,93,787
- 3. Leckel, D (2009) Diesel Production from Fischer-Tropsch: The Past, the Present, and New Concepts. Energy Fuels 23:2342-2358. Doi:10.1021/ef900064c
- 4. Hindermann JP, Hutchings GJ, and Kiennemann A (1993) Mechanistic Aspects of the Formation of Hydrocarbons and Alcohols from CO Hydrogenation. Cat Rev Sci and Eng 35:1–127
- 5. Dean, JA (1972) Lange's Handbook of Chemistry. McGraw Hill, New York
- 6. Xiaoding X, Doesburg EBM, Scholten JJF (1987) Synthesis of Higher Alcohols from Syngas Recently Patented Catalysts and Tentative Ideas on the Mechanism. Catal Today 2:125–170. Doi:10.1016/0920-5861(87)80002-0
- 7. Pan X, Fan Z, Chen WEI, Ding Y, Luo H, and Bao X (2007) Enhanced Ethanol Production inside Carbon-Nanotube Reactors Containing Catalytic Particles. Nat Mater 6:507-511. Doi:10.1038/nmat1916
- 8. Burch R, Petch MI (1992) Investigation of the Synthesis of Oxygenates from Carbon Monoxide / Hydrogen Mixtures on Supported Rhodium Catalysts. Appl Catal, A 88:39-60
- 9. Xiang M, Li D, Xiao H, Zhang J, Qi H, Li W, Zhong B, SunY (2008) Synthesis of Higher Alcohols from Syngas over Fischer Tropsch Elements Modified K/β -Mo<sub>2</sub>C Catalysts. Fuel 8:599–603. Doi:10.1016/j.fuel.2007.01.041
- 10. Luk HT, Mondelli C, Ferré DC, Stewart JA, and Pérez-Ramírez J (2017) Status and Prospects in Higher Alcohols Synthesis from Syngas. Chem Soc Rev 46:1358-1426
- 11. Schulz, H (1999) Short History and Present Trends of Fischer–Tropsch Synthesis. Appl Catal A 186:3–12. Doi:10.1016/S0926-860X(99)00160-X
- 12. Forzatti P, Tronconi E, Pasquon I (1991) Higher Alcohol Synthesis. Cat Rev 33:109-168
- 13. Subramani V, Gangwal SK (2008) A Review of Recent Literature to Search for an Efficient Catalytic Process for the Conversion of Syngas to Ethanol. Energy Fuels 8:814–839
- 14. Fang K, Li D, Lin M, Xiang M, Wei W, Sun Y(2009) A Short Review of Heterogeneous Catalytic Process for Mixed Alcohols Synthesis via Syngas. Catal Lett 147:133–138. Doi:10.1016/j.cattod.2009.01.038
- 15. Woo HC, Park KY, Kim YG, Nam I, Shik J, Lee JS (1991) Mixed Alcohol Synthesis from Carbon Monoxide and Dihydrogen over Potassium-Promoted Molybdenum Carbide Catalysts. Appl Catal 75: 267–280
- 16. Zaman S, Smith KJ (2012) A Review of Molybdenum Catalysts for Synthesis Gas Conversion to Alcohols: Catalysts, Mechanisms and Kinetics. Cat Rev 54: 41–132

- 17. Luk HT, Mondelli C, Ferré DC, Stewart JA, Pérez-ramírez J (2017) Status and Prospects in Higher Alcohols Synthesis from Syngas. Chem Soc Rev 46:1358–1426. Doi:10.1039/C6CS00324A
- 18. Sugier A, Freund E (1978) Process for Manufacturing Alcohols, Particularly Linear Saturated Primary Alcohols, from Synthesis Gas. US Patent 4122110 A
- 19. Courty P, Durand D, Freund E, Sugier A (1982) C<sub>1</sub>-C<sub>6</sub> Alcohols from Synthesis Gas on Copper-Cobalt Catalysts. J Mol Catal 17:241–254. Doi:10.1016/0304-5102(82)85035-9
- 20. Xiang Y, Kruse N (2016) Cobalt-Copper Based Catalysts for Higher Terminal Alcohols Synthesis via Fischer-Tropsch Reaction. J Energy Chem 25: 895–906. Doi:10.1016/j.jechem.2016.09.014
- 21. Xiang Y, Kruse N (2016) Tuning the Catalytic CO Hydrogenation to Straight- and Long-Chain Aldehydes/alcohols and Olefins/paraffins. Nat Commun 7:13058. Doi:10.1038/ncomms13058
- 22. Xiang Y, Barbosa R, Li X, Kruse N (2015) Ternary Cobalt-Copper-Niobium Catalysts for the Selective CO Hydrogenation to Higher Alcohols. ACS Catal 5:2929–2934. Doi:10.1021/acscatal.5b00388
- 23. Zhong L, Yu F, An Y, Zhao Y, Sun Y, Li Z, Lin T, Lin Y, Qi X, Dai Y, Gu L, Hu J, Jin S, Shen Q, Wang H (2016) Cobalt Carbide Nanoprisms for Direct Production of Lower Olefins from Syngas. Nature 538:84–87. Doi:10.1038/nature19786
- 24. Collinge G, Xiang Y, Barbosa R, McEwen J-S, Kruse N (2016) CO-Induced Inversion of the Layer Sequence of a Model CoCu Catalyst. Surf Sci 648: 74–83. Doi:10.1016/j.susc.2015.10.014
- 25. Nishizawa T, Ishida K (1984) The Co-Cu (Cobalt-Copper) System. Bull APD 5:161–165. Doi:10.1520/D0850-11.1
- 26. Xiang Y, Barbosa R, Kruse N (2014) Higher Alcohols through CO Hydrogenation over CoCu Catalysts: Influence of Precursor Activation. ACS Catal 4: 2792–2800. Doi:10.1021/cs500696z
- 27. Beaumont SK, Alayoglu S, Pushkarev VV, Liu Z, Somorjai GA (2013) Exploring Surface Science and Restructuring in Reactive Atmospheres of Colloidally Prepared Bimetallic CuNi and CuCo Nanoparticles on SiO<sub>2</sub> in Situ Using Ambient Pressure X-Ray Photoelectron Spectroscopy. RSC 162: 31–44. Doi:10.1039/c2fd20145c
- 28. Sci C, Fischer P, Spivey JJ (2012) A DRIFTS Study of CO Adsorption and Hydrogenation on Cu-Based Core-Shell Nanoparticles. Catal Sci Tech 2:621–631. doi:10.1039/c2cy00413e
- 29. Musselwhite N, Brooks CJ, Marcus MA, Guo J, Liu Z, Kruse N, Somorjai GA (2013) Surface Composition Changes of Redox Stabilized Bimetallic CoCu Nanoparticles Supported on Silica under H<sub>2</sub> and O<sub>2</sub> Atmospheres and During Reaction between CO<sub>2</sub> and H<sub>2</sub>: In Situ X Ray Spectroscopic Characterization. Phys Chem C 117:21803-21809
- 30. Xiang Y, Chitry V, Liddicoat P, Felfer P, Cairney J, Ringer S, Kruse N (2013) Long-Chain Terminal Alcohols through Catalytic CO Hydrogenation. JACS 135:7114–7117. Doi:10.1021/ja402512r
- 31. Lebarbier VM, Mei D, Kim DH, Andersen A, Male JL, Holladay JE, Rousseau R, Wang Y (2011) Effects of La<sub>2</sub>O<sub>3</sub> on the Mixed Higher Alcohols Synthesis from Syngas over Co Catalysts: A Combined Theoretical and Experimental Study. J Phys Chem C 115:17440–17451. Doi:10.1021/jp204003q
- 32. Wang Z, Spivey JJ (2015) General Effect of ZrO<sub>2</sub>, Al<sub>2</sub>O<sub>3</sub> and La<sub>2</sub>O<sub>3</sub> on Cobalt Copper Catalysts for Higher Alcohols Synthesis. General App Catal, A 507: 75–81. Doi:10.1016/j.apcata.2015.09.032
- 33. Volkova GG, Yurieva TM, Plyasova LM, Naumova MI, Zaikovskii VI (2000) Role of the Cu-Co Alloy and Cobalt Carbide in Higher Alcohol Synthesis. J Mol Catal A: Chem 158: 389–393. Doi:10.1016/S1381-1169(00)00110-2
- 34. Pei YP, Liu JX, ZhaoYH, Ding YJ, Liu T, Dong WD, Zhu HJ, Su HY, Yan L, Li JL, Li WX (2015) High Alcohols Synthesis via Fischer-Tropsch Reaction at Cobalt Metal/carbide Interface. ACS Catal 5:3620–3624. Doi:10.1021/acscatal.5b00791
- 35. Yang Y, Qi X, Wang X, Dong Lv, Yu F, Zhong L, Wang H, Sun Y (2016) Deactivation Study of CuCo Catalyst for Higher Alcohol Synthesis via Syngas. Catal Today 270: 101–107. Doi:10.1016/j.cattod.2015.06.014
- 36. Cheng, J, Hu P, Ellis P, French S, Kelly G, Lok CM (2010) Density Functional Theory Study of Iron and Cobalt

Carbides for Fischer - Tropsch Synthesis. J Phys Chem C 114: 1085–1093.

- 37. Thompson K, Lawrence D, Larson DJ, Olson JD, Kelly TF, Gorman B (2007) In Situ Site-Specific Specimen Preparation for Atom Probe Tomography. 107: 131–139. Doi:10.1016/j.ultramic.2006.06.008
- 38. Xiang Y, Chitry V, Kruse N (2013) Selective Catalytic CO Hydrogenation to Short- and Long-Chain C<sub>2</sub>+ Alcohols. Catal Lett 143: 936–941. Doi:10.1007/s10562-013-1060-0
- 39. Chenakin SP, Szukiewicz R, Barbosa R, Kruse N (2016) Journal of Electron Spectroscopy and Surface Analysis of Transition Metal Oxalates: Damage Aspects. J Electron Spectrosc Relat Phenom 209: 66–77. Doi:10.1016/j.elspec.2016.04.001